Computational Simulation and Analysis of 3D Body Surface Potential Patterns Generated by Common Atrial Arrhythmias

Ana Ferrer[1], Rafael Sebastian[2], Jose F Rodriguez[3], Catalina Tobón[4], Maria Guillem[1], Eduardo J Godoy[1], Javier Saiz[1]

[1]Universidad Politécnica de Valencia, Valencia, Spain
[2]Universitat de Valencia, Valencia, Spain
[3]Universidad de Zaragoza, Zaragoza, Spain
[4] Universidad lTM-Robledo, Medellín, Colombia

Abstract

Atrial arrhythmias are the most common cardiac pathologies and the variety of mechanisms of onset and progression are not well understood.

This study proposes a set of indices able to characterize a normal sinus rhythm and discriminate between flutter, tachycardia and fibrillation. Attention was paid to the correlation between atrial sites with high frequency arrhythmic activity and the corresponding torso surface activity to help in the non-invasive diagnosis of electrical cardiac problems.

A 3D human torso model that includes an anatomically realistic atria model was used to obtain biophysical simulations of electrical atrial depolarization and surface potential maps. Dominant frequency, power spectral peak, spectral correlation, sample entropy and phase-space diagrams were studied and graphically represented by 3D maps to describe characteristic patterns.

These indices and gradients in surface maps revealed important dissimilarities in spatial and temporal distributions among different propagation patterns and allowed classifying each type of arrhythmia.

1. Introduction

Atrial arrhythmias and mainly atrial fibrillation (AF) are the most common cardiac disorders and the variety of mechanisms of onset and progression are not well understood. Furthermore, it has been reported that the ablation of high frequency sources in patients with AF could be an effective therapy to restore sinus rhythm [1]. However, the number of AF recurrences proved the need to identify sites with abnormal frequency activity in the atria that help to improve current planning and intervention therapies. On the other hand, ECG is still the non-invasive standard method for monitoring the activity of the heart. However, difficulties on ECG signal recording and interpretation, which depend on the clinician expertise and ability to diagnose, have motivated the development of multi-scale computer models for investigating the mechanisms that underlie atrial rhythm disturbances. The development of body surface potential mapping (BSPM) systems is offering novel non-invasive ways to explore the behaviour of atria. However, it is still very difficult to infer the exact location of the arrhythmia source or analyse its temporal behaviour from the surface body signals of BSPM.

Previous studies focused on the electrophysiological signal processing analysed dominant frequency (DF) [2, 3], atria-torso DF equivalence [4], entropy [5, 6] or phase-space plots [7]. However, the present study adjusts and combines all these indices calculated from both, the atria and the torso surfaces to help in the discrimination and characterization of normal sinus rhythm (SR) and three different types of arrhythmic atrial propagations - flutter (AFL), tachycardia (AT) and fibrillation (AF). In addition, spectral correlation between atrial sites with high frequency arrhythmic activity and the corresponding torso surface signal have been studied.

2. Material and methods

2.1. Anatomical model

Data to build the 3D torso model was obtained from a CT scan collected at Utah University [8]. Relevant organs from the torso (lungs, bones, liver, ventricle, blood pools, and flesh) were reconstructed by threshold segmentation and manually corrected. A tetrahedral solid mesh (Figure 1 left), with 134.600 nodes and 754.394 elements with a resolution of 0.6mm was generated for the whole torso and conductivity values were assigned organs The original atrial model replaced by our detailed anatomical model described in [3] (Figure 1 right).

2.2 Biophysical simulation

The Nygren ionic model of human atrial electrophysiology was used to simulate the action potentials. Physiological and electrical remodelled conditions were considered by adjusting different parameters of the cellular model as in [3].

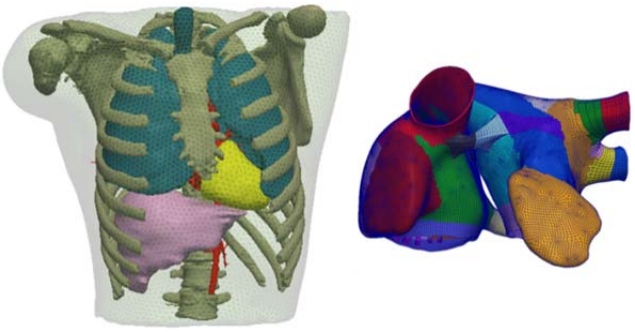

Figure 1. Left, torso model including lungs, bones, liver, ventricle, blood pools and flesh; Right, colour-coded atria model depending on the fibre direction.

The electrical propagation of the action potential through the atrial model and the passive propagation from the atria to the torso surface were performed using the mono-domain approach and the finite elements method to solve the reaction-diffusion system [9, 10].

The stimulation protocol consisted of a model stabilization phase of 10 continuous beats with a basic cycle length (BCL) of 1000ms, followed by another 10 beats with the same BCL in the case of sinus rhythm or 6 ectopic beats with a BCL of 130ms to generate a characteristic sustained re-entrant corresponding to AFL, AT or AF. The specific sites where these stimuli were applied were: sinoatrial node (SR), coronary sinus (AFL), crista terminalis (CT) and right pulmonary veins (AF).

2.3. Signal analysis

Simulated intracardiac surface electrograms (EGMs) were registered to analyse the atrial activity. These signals were pre-processed as described in [3, 4] and transformed to the spectral domain using the Welch periodogram with a Hamming window, 8 segments, 50% overlapping and 512 points for the Fast Fourier Transform (NFFT) to estimate the power spectral density (PSD). The frequency corresponding to the largest peak in the PSD between 1 and 10Hz was considered the atrial dominant frequency (DF). The DF value of each EGM was represented by a 3D colour-coded map on top of the atria surface (see Figure 2, first row).

In order to determine the DF at the torso surface, the Welch periodogram was also calculated on the surface electrocardiograms (ECGs). After that, a power threshold was applied to identify those PSD with a power spectral density contribution lower than 80% of the maximum which were set to 0 value (Figure 2, second row). The DF value of each ECG was represented by a 3D colour-coded map on top of the torso surface (Figure 2, third row).

Once DF was computed at the atria and torso, the spectral correlation (SC) was calculated in order to determine the relationship between all inside-outside pair of spectra. This SC coefficient represents the degree of linear dependence between each spectrum in the atria and each spectrum in the torso giving a value between +1 (total positive correlation) and -1 (negative correlation). In addition, a matrix of p-values for testing the hypothesis of no correlation was also obtained. Only SC coefficients higher than 98% of the maximum, and p-values smaller than 0.05, were considered as statistically significant.

The non-linear metric used to further characterize atrial arrhythmias was the sample entropy (SampEn), an improved method that reduces the shortcomings of the approximate entropy method [5, 11]. Briefly, SampEn is the negative natural logarithm of an estimate of the conditional probability that subseries of length m that match point wise within a tolerance r also match at the next point.

$$SampEn(m, r, N) = -\ln\left[\frac{A^m(r)}{B^m(r)}\right]$$

where N is the length of the signal, $A^m(r)$ represents the number of matches within that subseries, and $B^m(r)$ indicates the number of matches for the next point. Thus, the larger is the entropy, the more irregularity in the data, and the lower are the values, the more self-similarity.

The last index proposed to understand the behaviour of the arrhythmias under study was the phase analysis. This analysis allows to identify and quantify the spatial and temporal organization of a SR or arrhythmic events such as AFL, AT or AF. The phase-space plot of the time series was calculated using the Hilbert Transform $H[x(t)]$, which converts the original real signal x(t) into a new complex signal of type $z(t) = x(t) + jH[x(t)]$.

3. Results

Figure 2 shows the results obtained from the analysis of the DF, PSD and SC for the simulated (a) SR, (b) AFL, (c) AT and (d) AF. The lower row of the figure depicts the ECGs registered at the V1 precordial chest lead.

DFs calculated from the spectrum of the intracardiac EGMs in the atria (see Figure 2) revealed homogeneous patterns in SR, AFL and AT with the values shown in Table 1. However AF showed two well-defined regions with frequencies of 1.17Hz localized at the middle inferior free wall of the left atria and valves, and a range between 5.47Hz and 6.25Hz for the rest of the atria.

DFs calculated from the unipolar torso ECGs such as V1 (Figure 2 lower row), and restricted to the region with power contribution higher than 80% of the maximal are shown in Figure 2 second and third rows, respectively. Together with the values shown in Table 1, it can be observed that the DF in these regions was homogenous and similar to the DF at the atria surface in the four simulated cases.

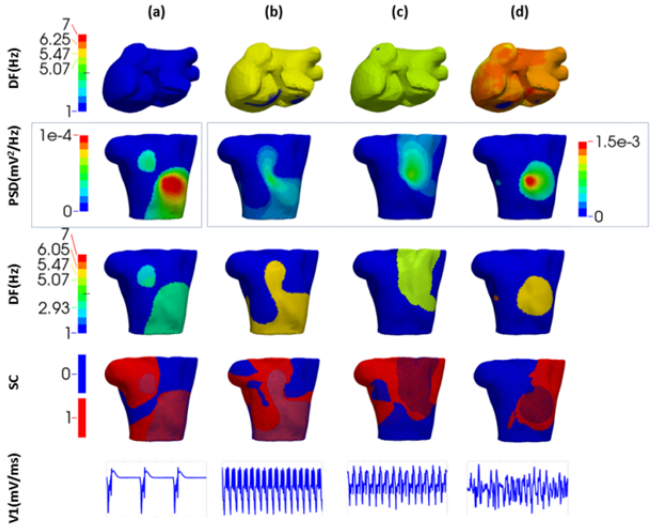

Figure 2: Row-wise: first dominant frequency at the atria (DF, Hz), second power spectral density peak (PSD, mV^2/ms), third spectral correlation (SC), and fourth precordial V1 chest lead (mV/ms). Column-wise: (a) Sinus Rrhtym SR, (b) Atrial Flutter AFL, (c) Atrial Tachycardia AT, (d) Atrial Fibrillation AF. PSD peak colour bar for (a) is located at the left side, whereas for (b), (c) and (d) is located at the right side.

Spectral correlation maps for all the simulated cases are shown in Figure 2 fourth row with its largest SC coefficients in Table 1. Red colour indicates positive correlation, whereas blue colour represents no or negative correlation. These red areas mostly coincide with the regions of the torso with high power contribution suggesting the pathway covered by the potential wave front at the torso surface.

Index	SR	AFL	AT	AF
DF_{ATRIA}	1.17	5.47	5.07	[1.17,6.25]
DF_{TORSO}	2.93	5.47	5.07	[5.47,6.05]
SC_{MAX}	0.9393	0.9998	0.9997	0.9993
SE_{ATRIA}	[0.002, 0.015]	[0.019, 0.254]	[0.016, 0.206]	[0.023, 0.253]
SE_{TORSO}	[0.009, 0.030]	[0.152, 0.523]	[0.249, 0.586]	[0.576, 1.133]

Table 1. DF (Hz) in atria and torso surfaces, largest spectral correlation between atria and torso, and SampEn (SE) values from the atrial EGMs and torso ECGs.

Figure 3 presents the results obtained from the non-linear analysis of the SampEn on the atria (SE_{ATRIA}) and the torso (SE_{TORSO}) signals and the phase analysis of the V1 chest leads for all the simulated cases (a) SR, (b) AFL, (c) AT and (d) AF. Besides, Table 1 shows the SampEn ranges for both domains.

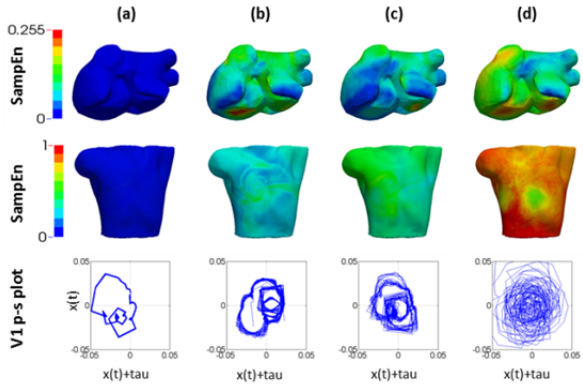

Figure 3: Row-wise: first sample entropy (SampEn) at the atria surface, second SampEn at the torso surface, third phase-space plots calculated from the V1 chest leads. Column-wise: (a) Sinus Rhythm SR, (b) Atrial Flutter AFL, (c) Atrial Tachycardia AT, (d) Atrial Fibrillation AF.

The SampEn values obtained on the atria and torso surfaces and its graphical representation in 3D colour-coded maps revealed a high regularity all over the surfaces with low entropy values in the case of SR. The cases of AFL and AT revealed higher entropy values, suggesting signal irregularity but distributed with certain homogeneity along the torso. The case of AF highlighted higher irregularity with the highest values of SampEn in both the atria and torso. Moreover, this last case seems to point out a concentration of medium entropy values in a circular area in the middle front of the torso surface.

The phase-space plots corresponding to V1 precordial chest leads showed a well-defined trajectory around an attractor point in the case of SR, a unique but wider trajectory and thus more variability in AFL, an intensified dispersion in AT and a completely undefined trajectory spreading all over the space in the case of AF.

4. Discussion and conclusions

DF's obtained using biophysical simulations were in agreement with experimental measurements published in the literature [2, 4, 12] for both, the atria and the torso surfaces. The main differences between both domains may be due to the effect introduced by the torso as a passive conductor. Thus, the DF in the torso not only responds to atrial activity but also to the propagation through the torso itself. Besides, if the torso area with high correlation regarding the atria is overlapped with the

torso area with high power contribution (see gridded red area in Figure 2 fourth row), the new defined region seems to correspond to the pathway covered by the potential wave front at the torso surface. Thus, the gridded area for each simulated case could be the best specific location to register the normal atrial activity or the specific arrhythmia, depending on the case.

The results obtained from the entropy analysis were as expected. When the arrhythmia becomes irregular (from AFL and AT to AF), the mean value of the SampEn increases in both the atria and torso. The case of AF additionally revealed that the region with high correlation inside-outside and a high power contribution was nearly the same with the middle SampEn value registered (green coloured region in Figure 3 (d) middle row). Thus, SampEn could be a good indicator for clinicians to detect and better characterize AF and the green circular region the best torso position to locate the electrodes.

Finally, phase-space plots facilitate classifying the type of electrical propagation as SR or arrhythmia, and between different arrhythmic activities. However a more in depth analysis has yet to be done regarding the trajectories obtained, the centre of the attractor, the diameter of the curve and how much disperse is this trajectory.

In conclusion, the numerical indicators and 3D colour maps calculated on the atria and torso surfaces revealed important differences in spatial distributions of power, dominant frequencies and sample entropy values among the different rhythms. Thus, these parameters allow classifying and characterizing each type of arrhythmia. Moreover, combining the results obtained through DF, spectral correlation and sample entropy it could be possible to define a region on the torso surface where clinicians could better detect and diagnose each type of arrhythmia.

Acknowledgements

This study is partly supported by the eTorso project (GV/2013/094) from Generalitat Valenciana, the project SAFE-PLAI (TIN2011-28067) from the Spanish Ministry of Science and Innovation, the project (TIN2012-37546-C03-01) from the “VI Plan Nacional de Investigación Científica, Desarrollo e Innovación Tecnológica” of the Spanish Ministry of Science and Innovation and the European Commission (European Regional Development Funds – ERDF - FEDER) and by the Programa Prometeo (PROMETEO/2012/030) of the Consellería d'Educació Formació I Ocupació, Generalitat Valenciana.

References

[1] Haissaguerre M, Jais P, Shah DC, Garrigue S, Takahashi A, Lavergne T, et al. Electrophysiological end point for catheter ablation of atrial fibrillation initiated from multiple pulmonary venous foci. Circulation 2000;101(12):1409-17. Epub 2000/03/29.

[2] Atienza F, Almendral J, Jalife J, Zlochiver S, Ploutz-Snyder R, Torrecilla EG, et al. Real-time dominant frequency mapping and ablation of dominant frequency sites in atrial fibrillation with left-to-right frequency gradients predicts long-term maintenance of sinus rhythm. Heart rhythm : the official journal of the Heart Rhythm Society 2009;6(1):33-40.

[3] Tobon C, Ruiz-Villa CA, Heidenreich E, Romero L, Hornero F, Saiz J. A three-dimensional human atrial model with fiber orientation. Electrograms and arrhythmic activation patterns relationship. PloS one 2013;8(2):e50883.

[4] Guillem MS, Climent AM, Millet J, Arenal Á, Fernández-Avilés F, Jalife J, et al. Noninvasive localization of maximal frequency sites of atrial fibrillation by body surface potential mapping. Circulation: Arrhythmia and Electrophysiology 2013;6(2):294-301.

[5] Pincus SM. Approximate entropy as a measure of system complexity. Proceedings of the National Academy of Sciences of the United States of America 1991;88(6):2297-301.

[6] Richman JS, Moorman JR. Physiological time-series analysis using approximate entropy and sample entropy. American Journal of Physiology - Heart and Circulatory Physiology 2000;278(6):H2039-H49.

[7] Roberts F, Povinelli R, Ropella K. Identification of ECG arrhythmias using phase space reconstruction. In: Raedt L, Siebes A, editors. Principles of Data Mining and Knowledge Discovery: Springer Berlin Heidelberg; 2001: 411-23.

[8] MacLeod RS, Johnson CR, Ershler PR. Construction of an Inhomogeneous Model of the Human Torso for Use in Computational Electrocardiography. IEEE Engineering in Medicine and Biology Society 13th Annual International Conference: IEEE Press 1991: 688-9.

[9] Heidenreich EA, Ferrero JM, Doblare M, Rodriguez JF. Adaptive macro finite elements for the numerical solution of monodomain equations in cardiac electrophysiology. Ann Biomed Eng 2010;38(7):2331-45.

[10] Rogers JM, McCulloch AD. A collocation--Galerkin finite element model of cardiac action potential propagation. IEEE Trans Biomed Eng 1994;41(8):743-57.

[11] Alcaraz R, Rieta JJ. A review on sample entropy applications for the non-invasive analysis of atrial fibrillation electrocardiograms. Biomedical Signal Processing and Control 2010;5(1):1-14.

[12] Millet-Roig J, Rieta JJ, Zarzoso V, Cebrian A, Castells F, Sanchez C, et al., editors. Surface-ECG atrial activity extraction via blind source separation: spectral validation. Computers in Cardiology 2002.

Address for correspondence:

Ana Ferrer Albero
Instituto Interuniversitario de Investigación en Bioingeniería y Tecnología Orientada al Ser Humano (UPV). Ciudad Politécnica de la Innovación (Cubo Azul, Edif. 8B). Camino de Vera s/n, 46022 - Valencia (Spain).
anferal0@upvnet.upv.es